

Near infrared fluorescent probes based on quinoxaline skeleton for imaging nucleic acid in mitochondria

Hai-Yan Peng,^a Gang Zhang,^b Yu-Jie Xu,^b Ru Sun,^{a,*} Jian-Feng Ge^{a,*}

^a College of Chemistry, Chemical Engineering and Material Science, Soochow University, 199 Ren' Ai Road, Suzhou 215123, China.

^b State Key Laboratory of Radiation Medicine and Protection, School of Radiation Medicine and Protection and Collaborative Innovation Center of Radiation Medicine of Jiangsu Higher Education Institutions, Soochow University, Suzhou 215123, China.

Index

| | |
|--|---|
| Table S1. Basic optical properties of common nucleic acid dyes and their targeting site in cells. | 3 |
| Table S2. Optical properties of probe 1a-c in different solvents. | 3 |
| Fig. S1. Photofading behaviours of probes 1a-c and Cy7 in acetonitrile. | 4 |
| Fig. S2. Optical properties of probe 1b (10 μ M) in different solvents. (a) Absorption spectra; (b) emission spectra (excited at 556 nm, slit widths: 3 nm/1.5 nm); (c) photographs under daylight; (d) photographs under a lamp at 365 nm in dark room. | 4 |
| Fig. S3. The electron cloud profiles of frontier molecular orbitals for probes 1a-b in cationic form and dye 1c calculated at the level of DFT//b3lyp/6-31g(d) using Gaussian software.. | 5 |
| Fig. S4. Excitation spectra of probe 1a | 6 |
| Fig. S5. Excitation spectra of probe 1b | 6 |
| Fig. S6. Optical responses of probe 1b (10 μ M) toward DNA (0–600 μ g/mL) in Tris–HCl buffer (10 mM, pH=7.4) containing 1% DMSO. (a)Absorption spectra; (b) emission spectra (λ_{ex} =590 nm, slit widths: 3 nm/5 nm); (c) fluorescence intensity toward different concentrations of DNA at 661 nm; (d) linear relationship of fluorescence intensity at 661 nm versus the concentration of DNA (0–350 μ g/mL). | 7 |
| Fig. S7. Optical responses of probe 1b (10 μ M) toward RNA (0–600 μ g/mL) in Tris–HCl buffer (10 mM, pH=7.4) containing 1% DMSO. (a)Absorption spectra of probe 1b in the presence of different concentrations of RNA (0–600 μ g/mL); (b)emission spectra (λ_{ex} =594 nm, slit widths: 3 nm/5 nm); (c) fluorescence intensity toward different concentrations of RNA at 663 nm; (d) | |

| | |
|--|----|
| linear relationship of fluorescence intensity at 663 nm versus the concentration of RNA (0–350 $\mu\text{g}/\text{mL}$); | 7 |
| Fig. S8. Selectivity experiments of probe 1b (10 μM) toward different analytes. Analytes: DNA (600 $\mu\text{g}/\text{mL}$), RNA (600 $\mu\text{g}/\text{mL}$), NADH (500 $\mu\text{g}/\text{mL}$), BSA (600 $\mu\text{g}/\text{mL}$), 5 mM for Ca^{2+} , Mg^{2+} , Mn^{2+} , Ni^{2+} , Cd^{2+} , Ba^{2+} ; 1 mM for S^{2-} , SO_3^{2-} , HSO_3^- ; 10 mM for K^+ , Na^+ , SCN^- , Cys, Gly, Hcy, Phe, His and Pro. ($\lambda_{\text{ex}}=594$ nm, slit widths: 3 nm/5 nm). | 8 |
| Fig. S9. Selectivity experiments of probe 1c (10 μM) toward different analytes. Analytes: DNA (600 $\mu\text{g}/\text{mL}$), RNA (600 $\mu\text{g}/\text{mL}$), 5 mM for Ca^{2+} , Ba^{2+} ; 1 mM for SO_3^{2-} , CO_3^{2-} , Cl^- ; 10 mM for Na^+ , Gly, GSH, Hcy, Phe and His. ($\lambda_{\text{ex}}=384$ nm, slit widths: 5 nm/5 nm). | 8 |
| Fig. S10. HeLa cells viabilities after treatment with probes 1a-c . Cell viability was assayed by the CCK-8 method. | 8 |
| Fig. S11. Fluorescence confocal images of living HeLa cells with probe 1b and ROI analysis: (a) bright field image; (b) confocal image (red channel) of cells with probe 1b (5 μM); (c) confocal image (green channel) of cells with Mito-Tracker Green FM (100 nM); (d) merged image of the green and red channels; (e) fluorescence intensity correlation plot of the green and red channels; (f) fluorescence intensities of the regions of interest (ROIs) across the cells..... | 9 |
| Fig. S12. Fluorescence confocal images of living HeLa cells with dye 1c and ROI analysis: (a) bright field image; (b) confocal image (green channel) of cells with dye 1c (5 μM); (c) confocal image (red channel) of cells with Mito-Tracker Red CMXRos (100 nM); (d) merged image of the green and red channels; (e) fluorescence intensity correlation plot of the green and red channels; (f) fluorescence intensities of the regions of interest (ROIs) across the cells. | 9 |
| Fig. S13. Fluorescence confocal images of the digest experiment for probe 1b (5 μM) with fixed HeLa cells. (a) Cells were incubated with 1b in control experiments; (b) cells were incubated with 1b and DNase (1 mg/mL); (c) cells were incubated with 1b and RNase (10 mg/mL). Red channel emission was collected in 570–750 nm upon excitation at 561 nm. | 10 |
| Fig. S14. ^1H NMR spectrum of probe 1a | 10 |
| Fig. S15. ^1H NMR spectrum of probe 1b | 11 |
| Fig. S16. ^1H NMR spectrum of dye 1c | 11 |
| Fig. S17. ^{13}C NMR spectrum of probe 1a | 12 |
| Fig. S18. ^{13}C NMR spectrum of probe 1b | 12 |
| Fig. S19. ^{13}C NMR spectrum of dye 1c | 13 |
| Fig. S20. HRMS (ESI $^+$) spectrum of probe 1a | 13 |
| Fig. S21. HRMS (ESI $^+$) spectrum of probe 1b | 14 |
| Fig. S22. HRMS (ESI $^+$) spectrum of dye 1c | 14 |

Table S1. Basic optical properties of common nucleic acid dyes and their targeting site in cells.

| Dyes | $\lambda_{\text{Abs,max}}^{\text{a}}$ | $\lambda_{\text{Em,max}}^{\text{a}}$ | Whether the dye can penetrate the cell membrane | Targeted subcellular organelle |
|----------------|---------------------------------------|--------------------------------------|---|--------------------------------|
| 1a (this work) | 561 ^b | 611 ^{b, c} | Yes | Mitochondria |
| SYBR Green I | 497 | 520 | Yes | Mitochondria and Nucleus |
| DAPI | 358 | 461 | Yes | Nucleus |
| Hoechst 33342 | 346 | 460 | Yes | Nucleus |
| PI | 493 | 636 | No | / |
| Gel Red | 510 | 600 | No | / |

^a Reported in nm. ^b Testing in DMSO. ^c Second highest emission peak.

Table S2. Optical properties of probes **1a-c** in different solvents.

| Probe | Solvents | $\lambda_{\text{Abs,max}}^{\text{a}}$ | $\lambda_{\text{Em,max}}^{\text{a}}$ | Stokes shift ^a | ϵ^{b} | Φ^{c} |
|-----------|-------------------|---------------------------------------|--------------------------------------|---------------------------|-----------------------|-------------------|
| 1a | H ₂ O | 503 | ND ^d | ND ^d | 2.3 | ND ^d |
| 1a | DMSO | 561 | 575 | 14 | 10.5 | 71.6 |
| 1a | MeOH | 560 | 578 | 18 | 10.2 | 86.9 |
| 1a | THF | 551 | 563 | 12 | 12.2 | 95.1 |
| 1a | DCM | 556 | 569 | 13 | 9.9 | 90.2 |
| 1a | TOL | 555 | 567 | 12 | 1.1 | 71.5 |
| 1b | H ₂ O | 505 | ND ^d | ND ^d | 1.0 | ND ^d |
| 1b | DMSO | 561 | 575 | 14 | 9.2 | 72.8 |
| 1b | MeOH | 560 | 575 | 15 | 8.5 | 78.8 |
| 1b | THF | 551 | 563 | 12 | 9.2 | 80.3 |
| 1b | DCM | 556 | 570 | 14 | 8.6 | 75.2 |
| 1b | TOL | 555 | 567 | 12 | 9.2 | 75.4 |
| 1c | H ₂ O | 373 | ND ^d | ND ^d | 0.9 | ND ^d |
| 1c | DMSO | 370 | 561 | 191 | 2.2 | 15.1 |
| 1c | EtOH | 369 | 575 | 206 | 3.2 | 9.4 |
| 1c | CHCl ₃ | 369 | 578 | 209 | 2.2 | 29.7 |
| 1c | THF | 366 | 562 | 196 | 2.4 | 21.2 |
| 1c | TOL | 368 | 560 | 192 | 2.4 | 31.4 |

^a Reported in nm. ^b Reported in 10⁴ M⁻¹ cm⁻¹. ^c Reported in %. ^d Reported in 'not detected'. Cresyl violet ($\Phi=0.578$ in ethanol) was used as the reference compound for **1a** and **1b**, coumarin-153 ($\Phi=0.544$ in ethanol) was used as the reference compound for **1c**.

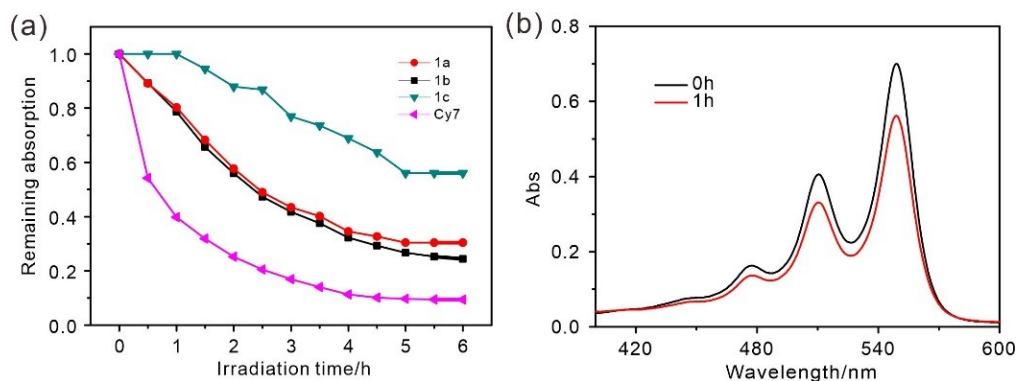


Fig. S1. Photofading behaviors of probes **1a-c** and Cy7 in acetonitrile. (a) The residual absorption rate of probes **1a-c** after continuous irradiation for 6 h; (b) absorption spectra of probe **1a** without irradiation and irradiation for 1 h.

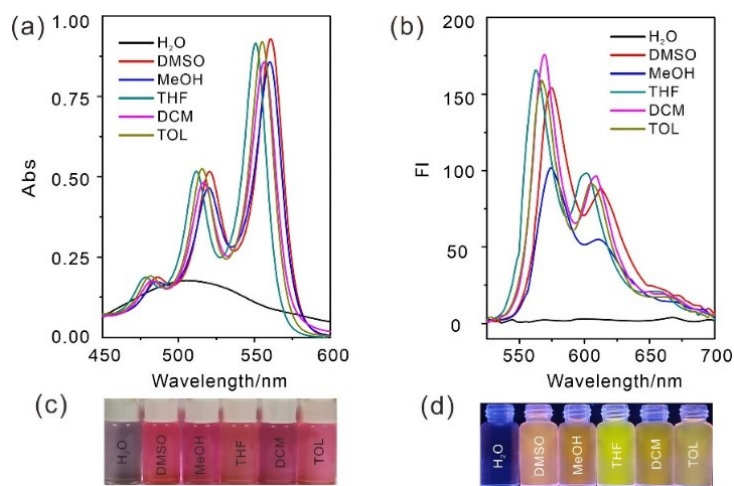


Fig. S2. Optical properties of probe **1b** (10 μ M) in different solvents. (a) Absorption spectra; (b) emission spectra (excited at 556 nm, slit widths: 3 nm/1.5 nm); (c) photographs under daylight; (d) photographs under a lamp at 365 nm in dark room.

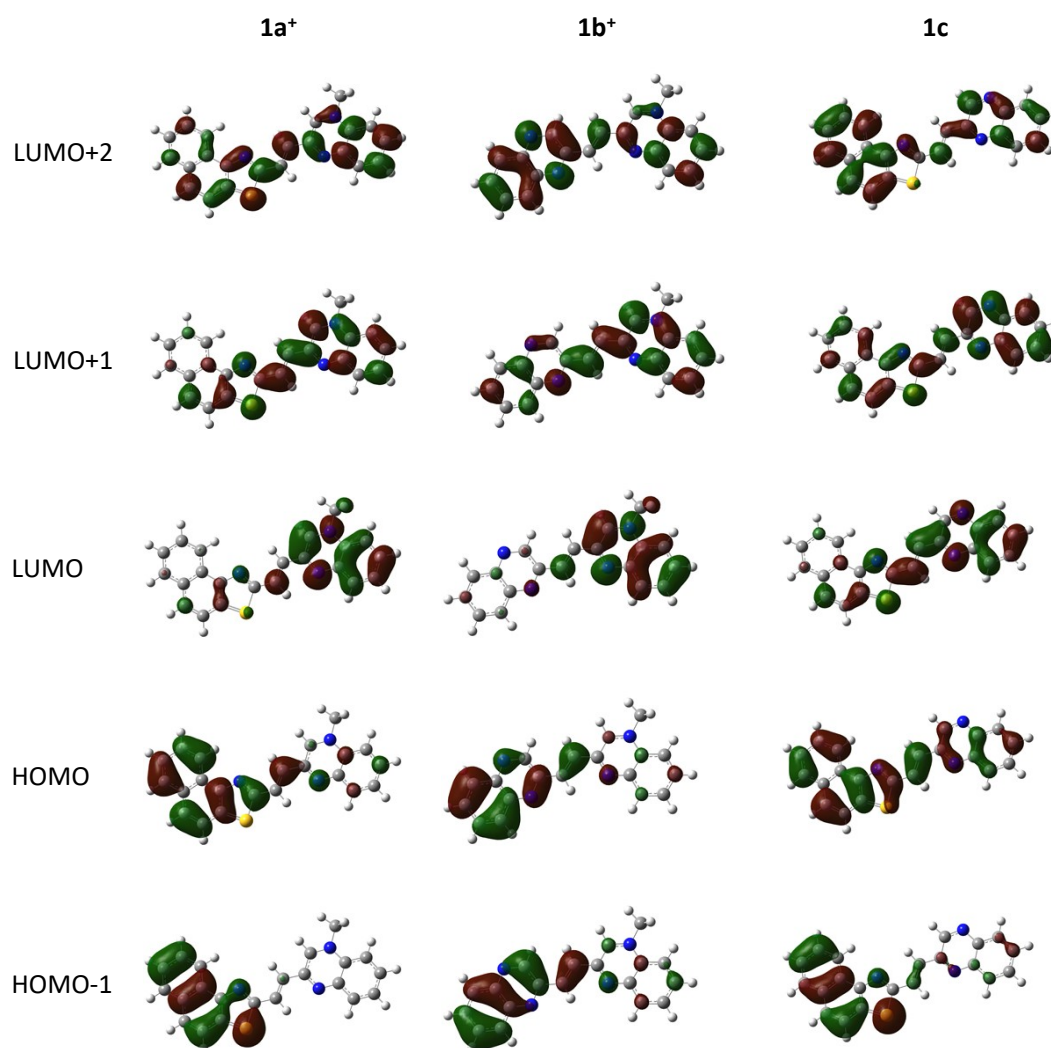


Fig. S3. The electron cloud profiles of frontier molecular orbitals for probes **1a-b** in cationic form and dye **1c** calculated at the level of DFT//b3lyp/6-31g(d) using Gaussian software.¹

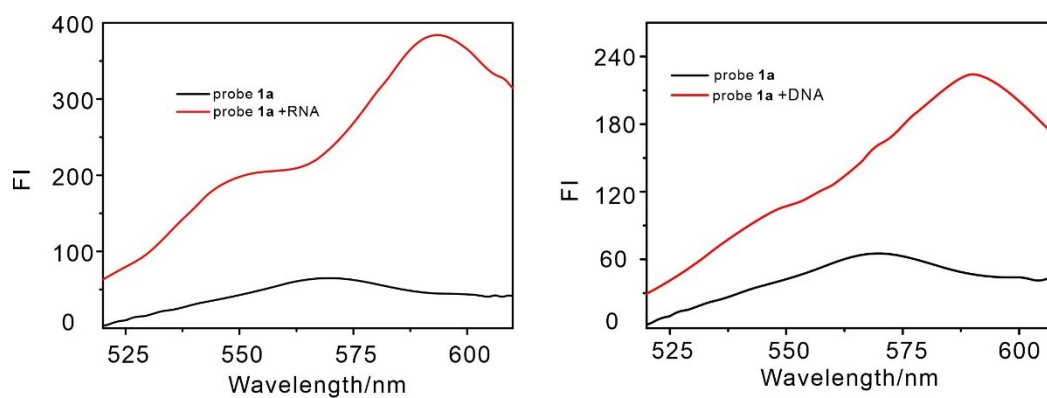


Fig. S4. Excitation spectra of probe **1a**.

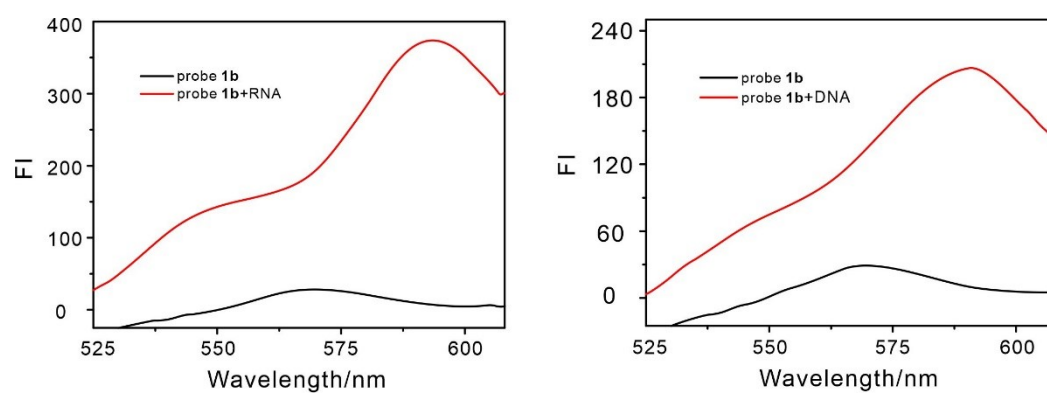


Fig. S5. Excitation spectra of probe **1b**.

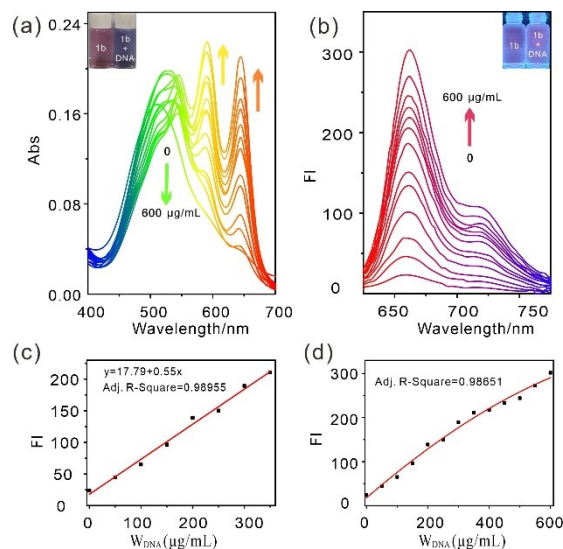


Fig. S6. Optical responses of probe **1b** (10 μM) toward DNA (0–600 $\mu\text{g/mL}$) in Tris–HCl buffer (10 mM, pH=7.4) containing 1% DMSO. (a) Absorption spectra; (b) emission spectra (λ_{ex} =590 nm, slit widths: 3 nm/5 nm); (c) linear relationship of fluorescence intensity at 661 nm versus the concentration of DNA (0–350 $\mu\text{g/mL}$); (d) fluorescence intensity toward different concentrations of DNA at 661 nm.

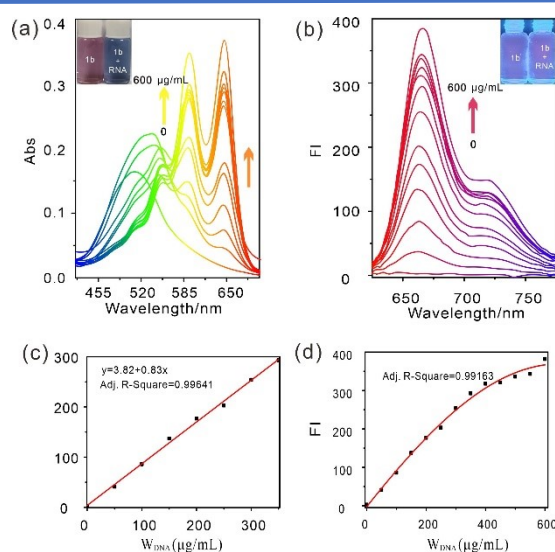


Fig. S7. Optical responses of probe **1b** (10 μM) toward RNA (0–600 $\mu\text{g/mL}$) in Tris–HCl buffer (10 mM, pH=7.4) containing 1% DMSO. (a) Absorption spectra; (b) emission spectra (λ_{ex} =594 nm, slit widths: 3 nm/5 nm); (c) linear relationship of fluorescence intensity at 663 nm versus the concentration of RNA (0–350 $\mu\text{g/mL}$); (d) fluorescence intensity toward different concentrations of RNA at 663 nm.

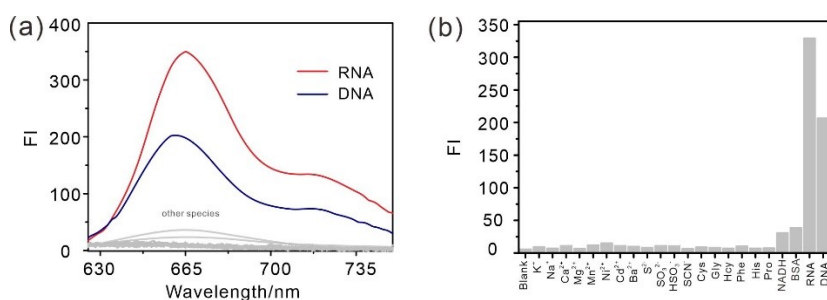


Fig. S8. Selectivity experiments of probe **1b** (10 μM) toward different analytes. Analytes: DNA (600 $\mu\text{g}/\text{mL}$), RNA (600 $\mu\text{g}/\text{mL}$), NADH (500 $\mu\text{g}/\text{mL}$), BSA (600 $\mu\text{g}/\text{mL}$), 5 mM for Ca^{2+} , Mg^{2+} , Mn^{2+} , Ni^{2+} , Cd^{2+} , Ba^{2+} ; 1 mM for S^{2-} , SO_3^{2-} , HSO_3^- ; 10 mM for K^+ , Na^+ , SCN^- , Cys, Gly, Hcy, Phe, His and Pro. ($\lambda_{\text{ex}}=594$ nm, slit widths: 3 nm/5 nm). (a)emission spectra; (b) fluorescence histogram at 660nm.

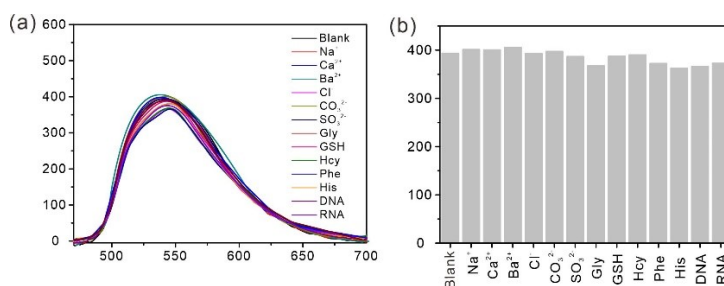


Fig. S9. Selectivity experiments of probe **1c** (10 μM) toward different analytes. Analytes: DNA (600 $\mu\text{g}/\text{mL}$), RNA (600 $\mu\text{g}/\text{mL}$), 5 mM for Ca^{2+} , Ba^{2+} ; 1 mM for SO_3^{2-} , CO_3^{2-} , Cl^- ; 10 mM for Na^+ , Gly, GSH, Hcy, Phe and His. ($\lambda_{\text{ex}}=384$ nm, slit widths: 5 nm/5 nm). (a)emission spectra; (b) fluorescence histogram at 550nm.

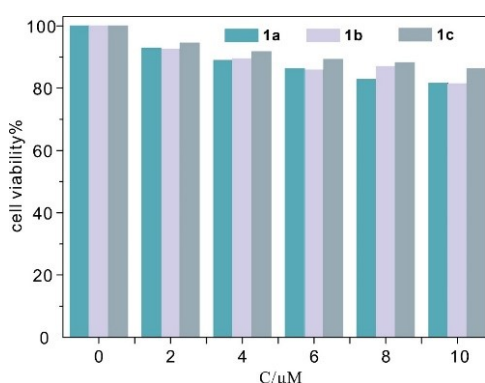


Fig. S10. HeLa cells viabilities after treatment with probes **1a-c**. Cell viability was assayed by the CCK-8 method.

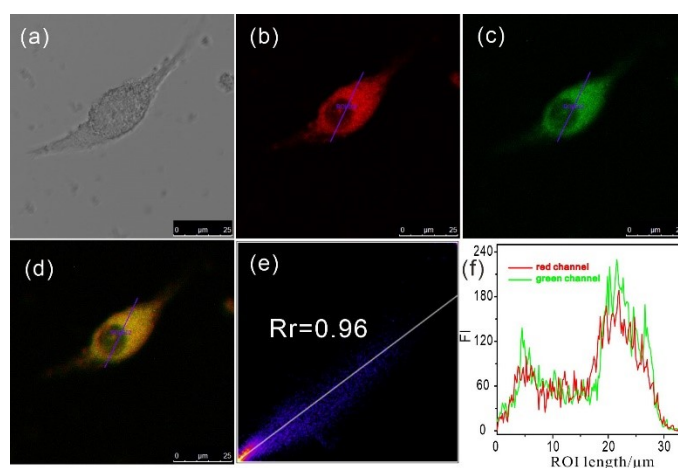


Fig. S11. Fluorescence confocal images of living HeLa cells with probe **1b** and ROI analysis: (a) bright field image; (b) confocal image (red channel) of cells with probe **1b** (5 μM); (c) confocal image (green channel) of cells with Mito-Tracker Green FM (100 nM); (d) merged image of the green and red channels; (e) fluorescence intensity correlation plot of the green and red channels; (f) fluorescence intensities of the regions of interest (ROIs) across the cells.

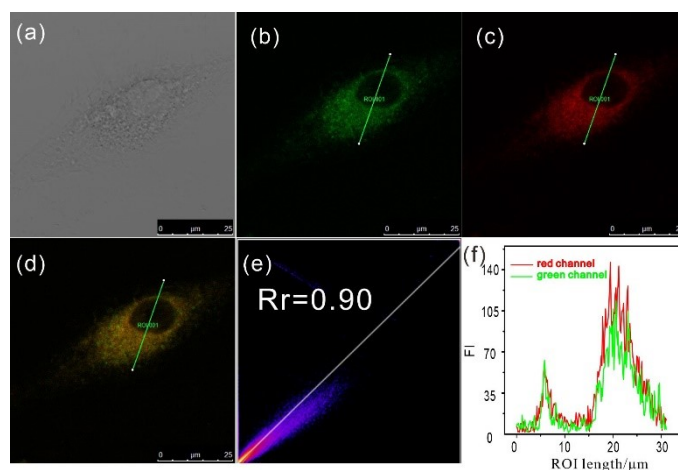


Fig. S12. Fluorescence confocal images of living HeLa cells with dye **1c** and ROI analysis: (a) bright field image; (b) confocal image (green channel) of cells with dye **1c** (5 μM); (c) confocal image (red channel) of cells with Mito-Tracker Red CMXRos (100 nM); (d) merged image of the green and red channels; (e) fluorescence intensity correlation plot of the green and red channels; (f) fluorescence intensities of the regions of interest (ROIs) across the cells.

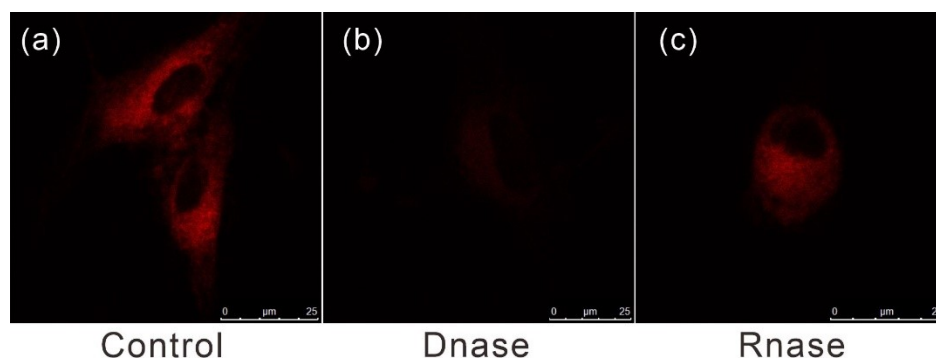


Fig. S13. Fluorescence confocal images of the digest experiment for probe **1b** (5 μM) with fixed HeLa cells. (a) Cells were incubated with **1b** in control experiments; (b) cells were incubated with **1b** and DNase (1 mg/mL); (c) cells were incubated with **1b** and RNase (10 mg/mL). Red channel emission was collected in 570–750 nm upon excitation at 561 nm.

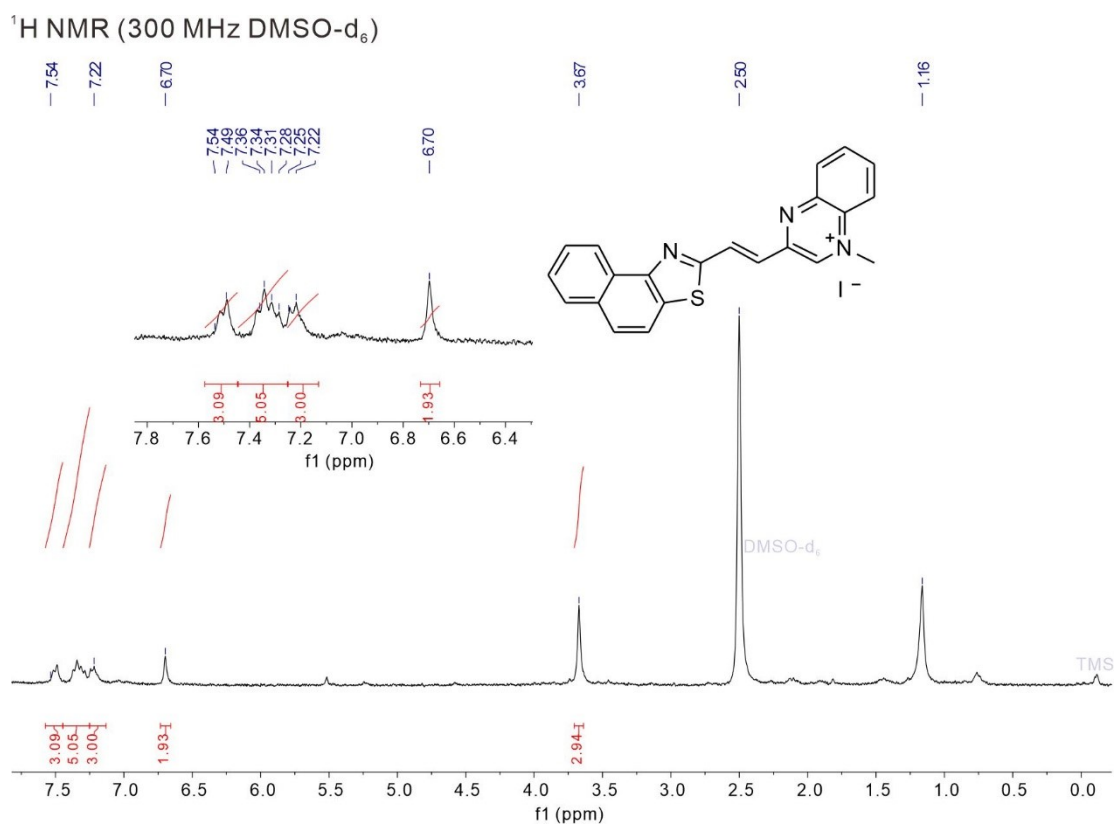
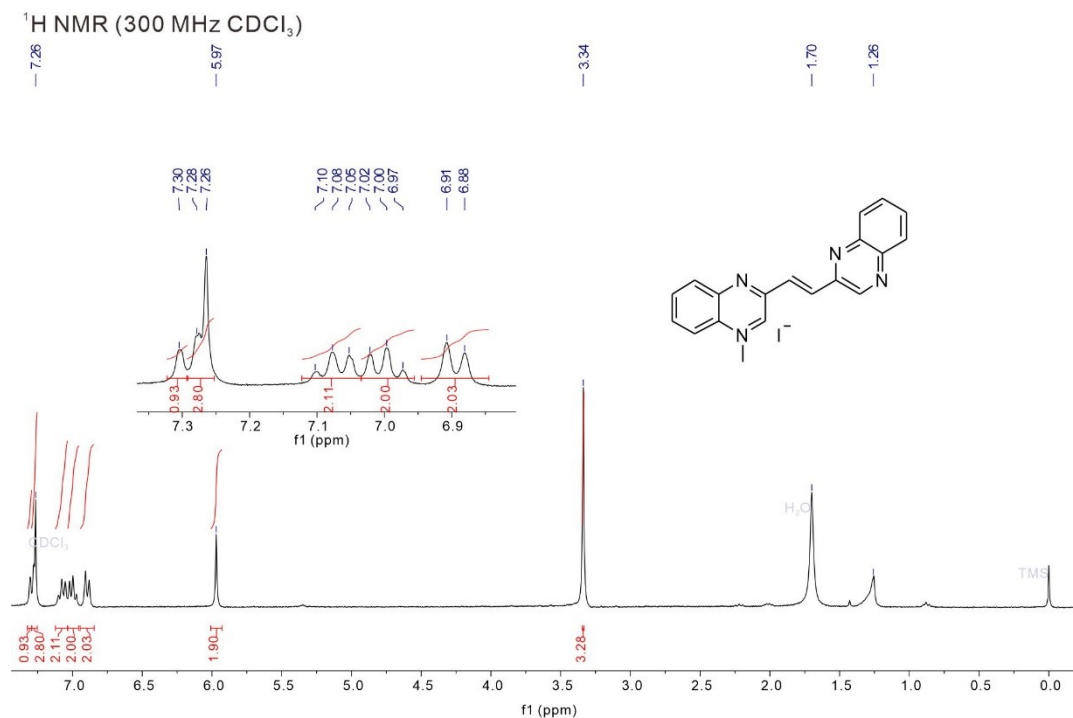
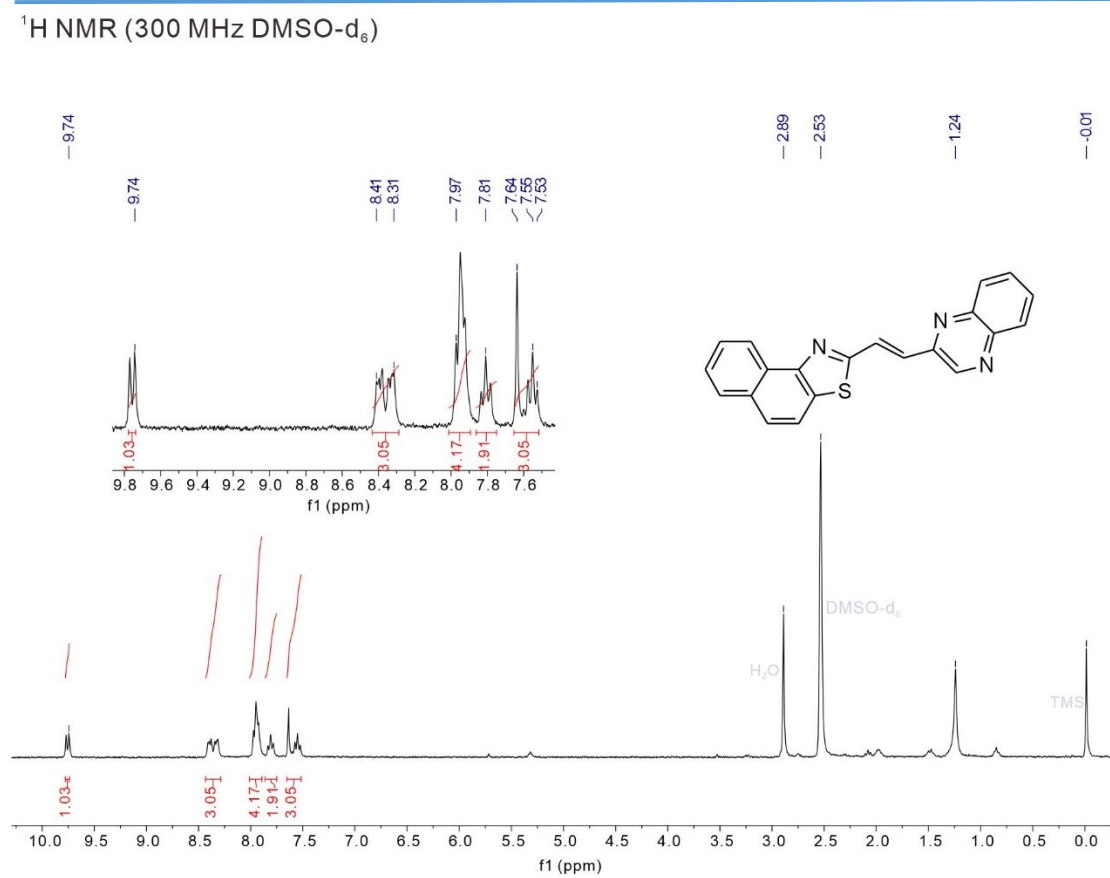
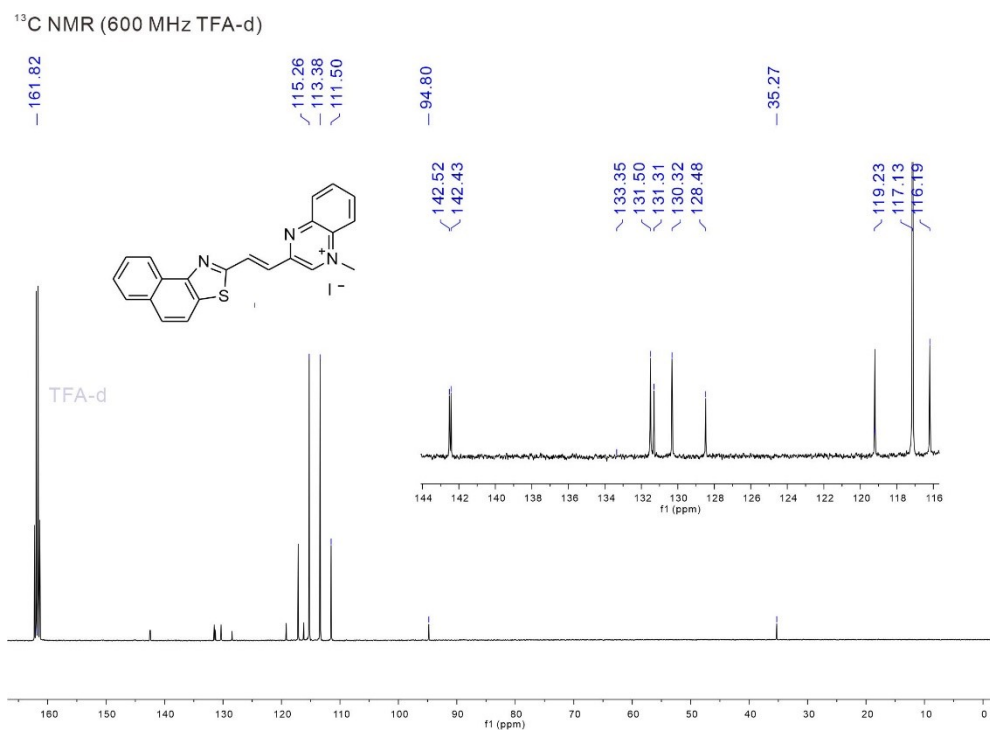
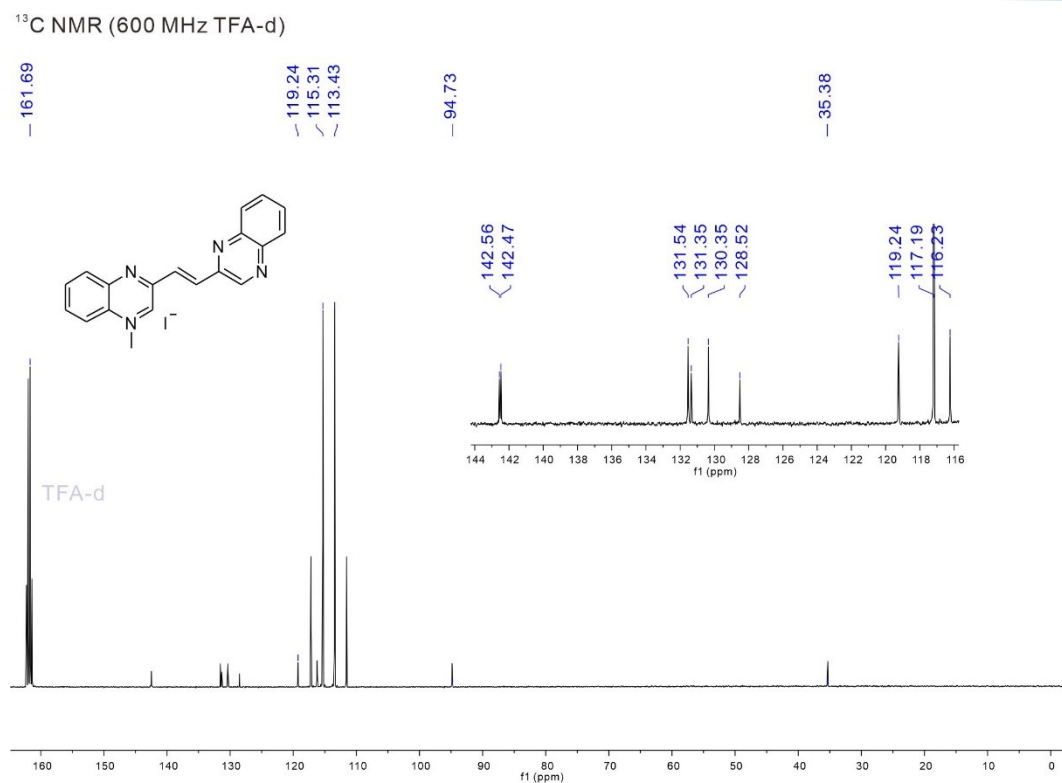
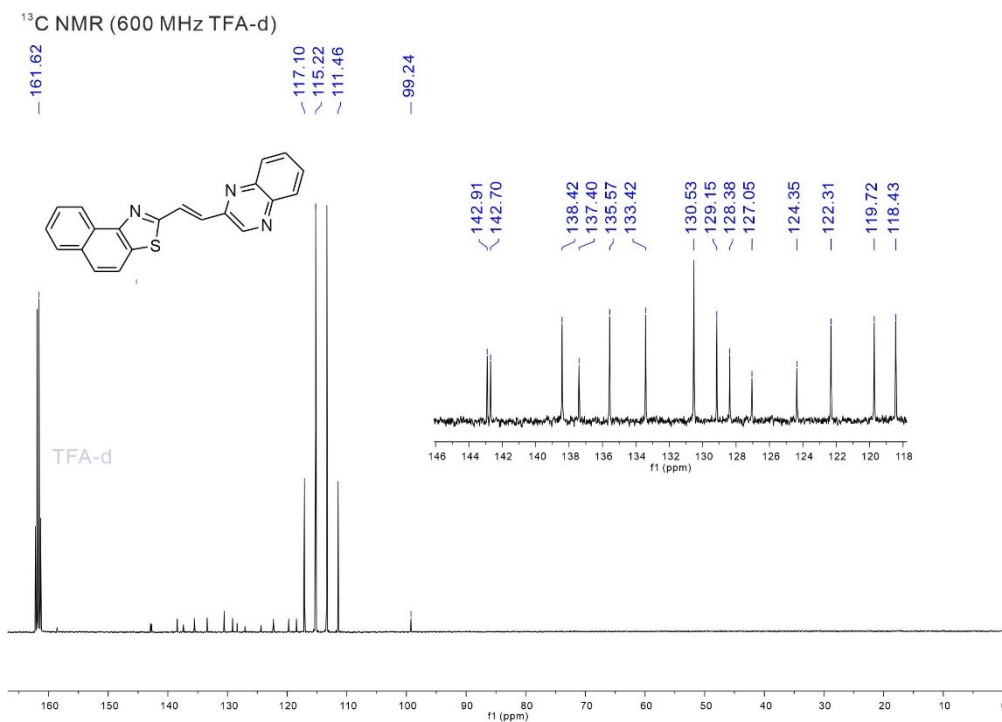


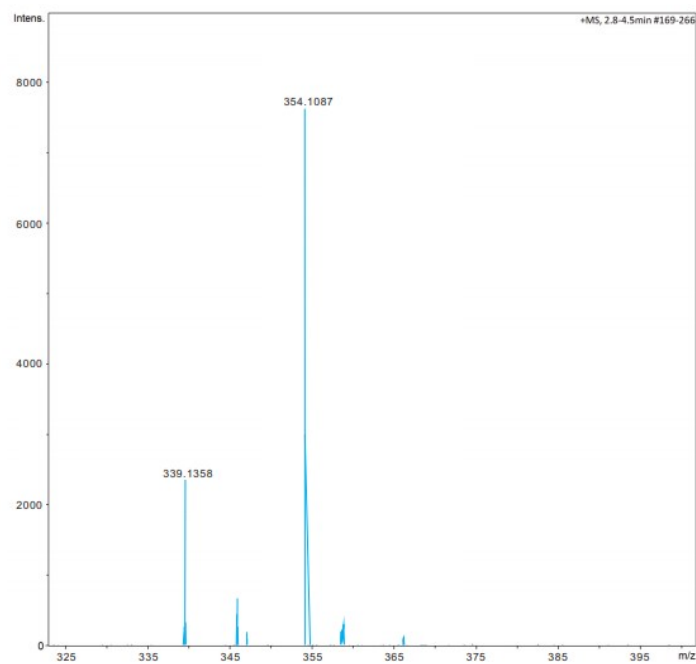
Fig. S14. ^1H NMR spectrum of probe **1a**.

**Fig. S15.** ^1H NMR spectrum of probe **1b**.**Fig. S16.** ^1H NMR spectrum of dye **1c**.

**Fig. S17.** ¹³C NMR spectrum of probe **1a**.**Fig. S18.** ¹³C NMR spectrum of probe **1b**.

Fig. S19. ¹³C NMR spectrum of dye 1c.

| Acquisition Parameter | | | | | |
|-----------------------|------------|-----------------------|-----------|------------------|-----------|
| Source Type | ESI | Ion Polarity | Positive | Set Nebulizer | 1.0 Bar |
| Focus | Not active | Set Capillary | 4500 V | Set Dry Heater | 180 °C |
| Scan Begin | 50 m/z | Set End Plate Offset | -500 V | Set Dry Gas | 4.0 l/min |
| Scan End | 3000 m/z | Set Collision Cell RF | 300.0 Vpp | Set Divert Valve | Waste |

Fig. S20. HRMS(ESI⁺) spectrum of probe 1a.

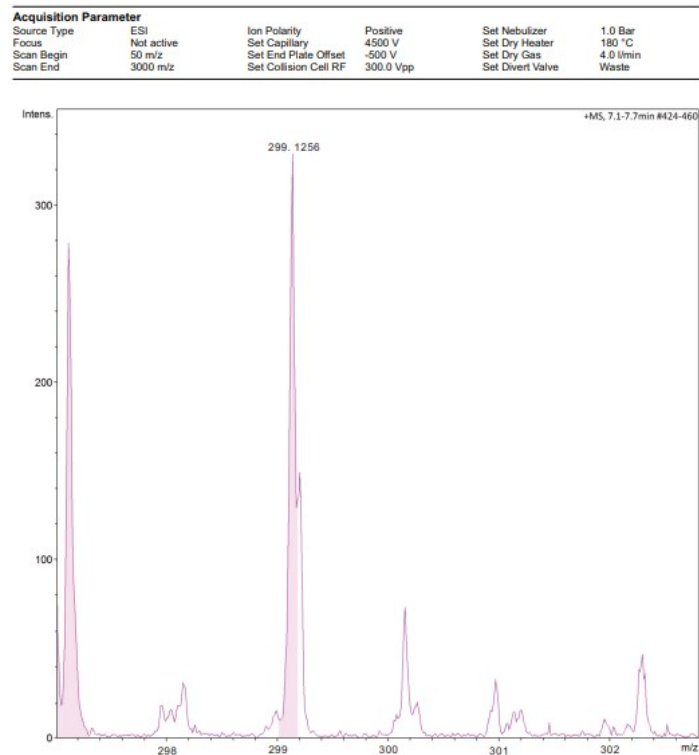


Fig. S21. HRMS(ESI⁺) spectrum of probe **1b**.

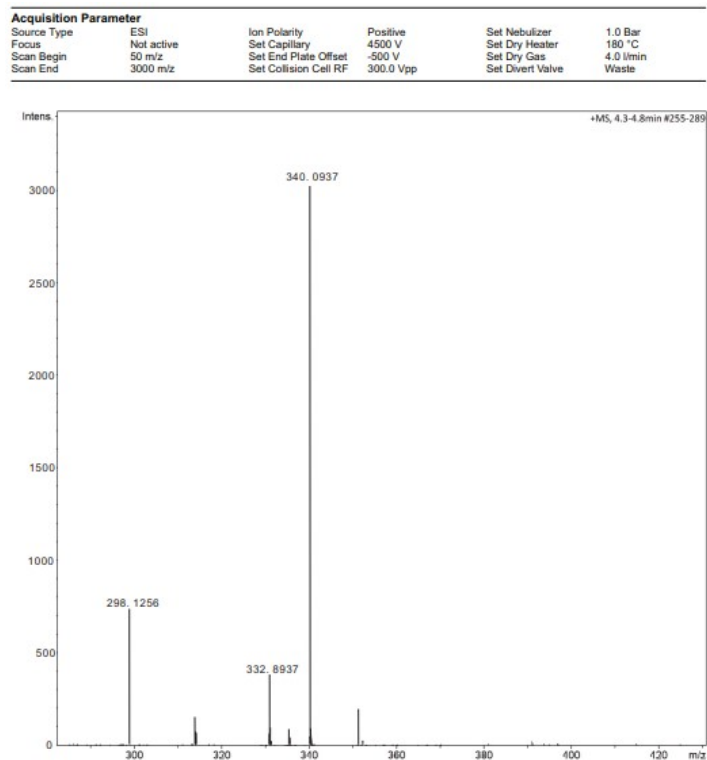


Fig. S22. HRMS(ESI⁺) spectrum of dye **1c**.

references

1. M. J. Frisch, G. W. Trucks, H. B. Schlegel, G. E. Scuseria, M. A. Robb, J. R. Cheeseman, G. Scalmani, V. Barone, B. Mennucci, G. A. Petersson, H. Nakatsuji, M. Caricato, X. Li, H. P. Hratchian, A. F. Izmaylov, J. Bloino, G. Zheng, J. L. Sonnenberg, M. Hada, M. Ehara, K. Toyota, R. Fukuda, J. Hasegawa, M. Ishida, T. Nakajima, Y. Honda, O. Kitao, H. Nakai, T. Vreven, J. A. Montgomery, Jr., J. E. Peralta, F. Ogliaro, M. Bearpark, J. J. Heyd, E. Brothers, K. N. Kudin, V. N. Staroverov, R. Kobayashi, J. Normand, K. Raghavachari, A. Rendell, J. C. Burant, S. S. Iyengar, J. Tomasi, M. Cossi, N. Rega, J. M. Millam, M. Klene, J. E. Knox, J. B. Cross, V. Bakken, C. Adamo, J. Jaramillo, R. Gomperts, R. E. Stratmann, O. Yazyev, A. J. Austin, R. Cammi, C. Pomelli, J. W. Ochterski, R. L. Martin, K. Morokuma, V. G. Zakrzewski, G. A. Voth, P. Salvador, J. J. Dannenberg, S. Dapprich, A. D. Daniels, O. Farkas, J. B. Foresman, J. V. Ortiz, J. Cioslowski, and D. J. Fox, Gaussian 09, Revision A.01, Gaussian, Inc., Wallingford CT, 2009.